Available online at www.sciencedirect.com
ScienceDirect
Advances in Space Research 45 (2010) 1156–1172
ADVANCES IN SPACE RESEARCH (a COSPAR publication)
www.elsevier.com/locate/asr

Application of Autoscala to ionograms recorded by the VIPIR ionosonde

T. Bullett [a], A. Malagnini [b], M. Pezzopane [b,*], C. Scotto [b]

[a] University of Colorado Cooperative Institute for Research in Environmental Sciences (CIRES), 325 Broadway, Boulder, CO 80305, USA
[b] Istituto Nazionale di Geofisica e Vulcanologia, Via di Vigna Murata 605, 00143 Rome, Italy

Received 4 August 2009; received in revised form 22 December 2009; accepted 16 January 2010

Abstract

In November 2008, the ionosonde station at Boulder, Colorado, USA (40.0°N; 105.3°W) became the host of a new ionosonde (VIPIR, Vertical Incidence Pulsed Ionospheric Radar) developed and built by Scion Associates.

The VIPIR is a fully digital frequency agile radar that operates between 0.3 and 26 MHz. It features 8 digital receivers and a digital transmit exciter. Extremely high performance analog receive electronics and a 4 kW solid state amplifier provide interface to the real world.

This work describes the application of Autoscala to the ionograms recorded by this ionosonde. First results, in terms of ionograms and autoscaled characteristics, are presented and discussed.

Keywords: Autoscala; Ionosphere; Ionogram; Electron density; Monitoring and modelling

1. Introduction

The process of scaling ionograms involves the determination of several numerical characteristics which define standard features of the ionogram data (Piggott and Rawer, 1972), such as the critical frequency of the F2 layer (*fo*F2). The ionograms from the ionosonde or High Frequency (HF) radar are, at a minimum, the amplitude of the received signals as a function of time of flight and sounding frequency. New research ionosondes can provide much more information than this (Wright and Bullett, 2003), but for the purpose of real time and long term monitoring of the ionosphere, the challenge of consistent, automatic scaling of ionograms into standard parameters remains an important objective. The improved data from a research ionosonde provides autoscaling software new opportunity and challenge.

2. Instrumentation

The Vertical Incidence Pulsed Ionospheric Radar (VIPIR) is a new design of ionosphere HF radar that was inspired by the capabilities of the 1980's NOAA HF radar (Grubb, 1979) and built with modern digital electronics (Grubb et al., 2008). It was developed by Scion Associates, supported by the US Air Force Research Laboratory and their Small Business Innovative Research Program. The radar consists of a 4 kW peak power solid state transmitter driven by a digital up-converter which generates precise amplitude and phase RF and a transmitted waveform amplitude. At Boulder, the high power pulses are transmitted toward the ionosphere using a 30 m tall delta antenna in use since the 1970's. This antenna, and the presence of several powerful broadcast transmitters in the area, limit the practical lower frequency of the instrument to 1.7 MHz at this location.

Signals returned from the ionosphere are received on an array of 8 horizontal dipole antennas. These are each 4 m total length, mounted 5 m above the ground. The receive

* Corresponding author. Tel.: +39 06 51860525; fax: +39 06 51860397.
E-mail addresses: Terry.Bullett@noaa.gov (T. Bullett), michael.pezzopane@ingv.it (M. Pezzopane).

0273-1177/$36.00 © 2010 COSPAR. Published by Elsevier Ltd. All rights reserved.
doi:10.1016/j.asr.2010.01.024

antennas at Boulder are equally spaced in a right handed Cartesian coordinate system, rotated 45 degrees from geographic North to accommodate field site space limitations. None of the direction of arrival observations theoretically possible with this antenna array are used in this study, so the orientation of the receive array with respect to the local magnetic field is not relevant for non-equatorial locations such as Boulder. Vertical propagation is assumed. The orthogonality of half the dipoles with respect to the other half is used for circular polarization observations.

The 8 receive antennas are connected to 8 digital receivers through a high performance analog front end. The analog portion consists of an impedance matching preamplifier mounted at the dipole feed point, phase matched receive signal cables, a receive antenna power and interface unit, an adjustable gain section and a low pass anti-aliasing filter with 26 MHz cutoff frequency. Band limited RF signals are presented to a set of eight 14-bit analog to digital converters sampling at 80 MHz. Full bandwidth digital data are presented to a digital down-converter which numerically downshifts the broadband data to a specific frequency and applies a programmable baseband filter. The raw baseband data are encoded into packets on a Universal Serial Bus (USB) interface and delivered to a control computer for capture and saving to files for each ionogram sweep. These files are on the order of 100 MB for each ionogram. The radar is controlled internally with several microcontrollers, which in turn are programmed by the general purpose control computer through the USB connections.

The raw files must be reduced into an ionogram useable by Autoscala. No precision range, arrival angle or Doppler calculations are performed, as these data are not required. Polarization of the received signals is used by Autoscala and is determined for each range gate by digital polarization synthesis. Two orthogonal circular polarizations are formed by numerically phase shifting by +90 and −90 degrees all the antennas pointing in one direction, and coherently adding these values to the values from the orthogonal antenna set. Both sets of amplitudes from the ordinary (O) and extraordinary (X) mode antenna configurations are recorded.

Incoherent averaging of the power from each IPP recorded at the same nominal frequency is performed. A statistical probability analysis is performed to estimate the noise level at each nominal frequency. A data file of netCDF format is created with full numerical resolution, and is then reformatted into a reduced size data file used by Autoscala. Full frequency and range data are retained, but amplitude information and metadata are reduced.

Numerous measurement modes are possible, but two standard modes have been used commonly. One is a full featured "Dynasonde B-mode" ionogram (Wright and Pitteway, 1979a,b) which runs 2.5 min every 5 min. The other is a fast sweep of 20 s duration that is repeated every minute. Autoscala's ability to analyze data from widely different modes gives scientific freedom to experiment with the radar for research purposes without compromising a routine ionosphere measurement capacity. These modes produce vast quantities of ionogram data at rates that cannot be practically analyzed by manual methods.

3. Autoscala and data input

Autoscala (Pezzopane and Scotto, 2005; Scotto and Pezzopane, 2002) is a program able to perform an automatic scaling of vertical soundings, giving as output the main ionospheric characteristics and an estimation of the electron density profile (Scotto, 2009). It is based on an image recognition technique and can run without polarization information, which allows the algorithm to be applied to any kind of ionosonde.

Autoscala works using ionograms as input in the form of binary files with the extension RDF (Pezzopane, 2004), hence in order to apply Autoscala to the ionograms recorded by the VIPIR ionosonde, a change of file format was required. After performing this format change, the file processed by Autoscala is a binary file whose name is BD840_*yyyydddhhmm*.RDF, where BD840 is the URSI code of the Boulder ionospheric station where the VIPIR ionosonde is installed, *yyyy* are the four digits for the year, *ddd* are the three digits for the calendar day, *hh* identifies the hour and *mm* the minutes. For each sounding frequency the information on the received energy is stored in two consecutive records of 512 bytes, the first one for the O mode and the other one for the X mode. The value of the first byte represents the noise level for that frequency and for that mode. The value of the second byte represents the energy reflected back towards the ground from a height of −2.3 km, byte 512 represents the energy reflected back towards the ground from a height of 762.2 km, such that the passage between two successive bytes of the record is equal to a step in height of 1.5 km.

The ionogram is memorized by Autoscala as two matrices A_{ord} and A_{ext} whose row and column numbers depend on the sounding settings as described in Pezzopane and Scotto (2007). The matrix element is an integer related to the echo amplitude received by the ionosonde, in decibels (dB) above the receiver sensitivity threshold. To consider an a_{ord} matrix element to be a potential echo, the following condition

$$a_{ord} - a_{ext} > 3\text{dB}$$

has to stand between it and the corresponding a_{ext} matrix element; analogously to consider an a_{ext} matrix element to be a potential echo, the following condition

$$a_{ext} - a_{ord} > 3\text{dB}$$

has to stand between it and the corresponding a_{ord} matrix element. In both cases the matrix element has to be greater than the noise level characterizing the considered frequency.

These matrices are then filtered to eliminate the traces caused by second-order reflection from ionograms (Scotto and Pezzopane, 2008).

Empirical curves, that are able to fit the typical shape of the F2, F1, and Es (Pezzopane and Scotto, 2007, 2008; Scotto and Pezzopane, 2007) trace, are then defined for the detection of the ionogram trace.

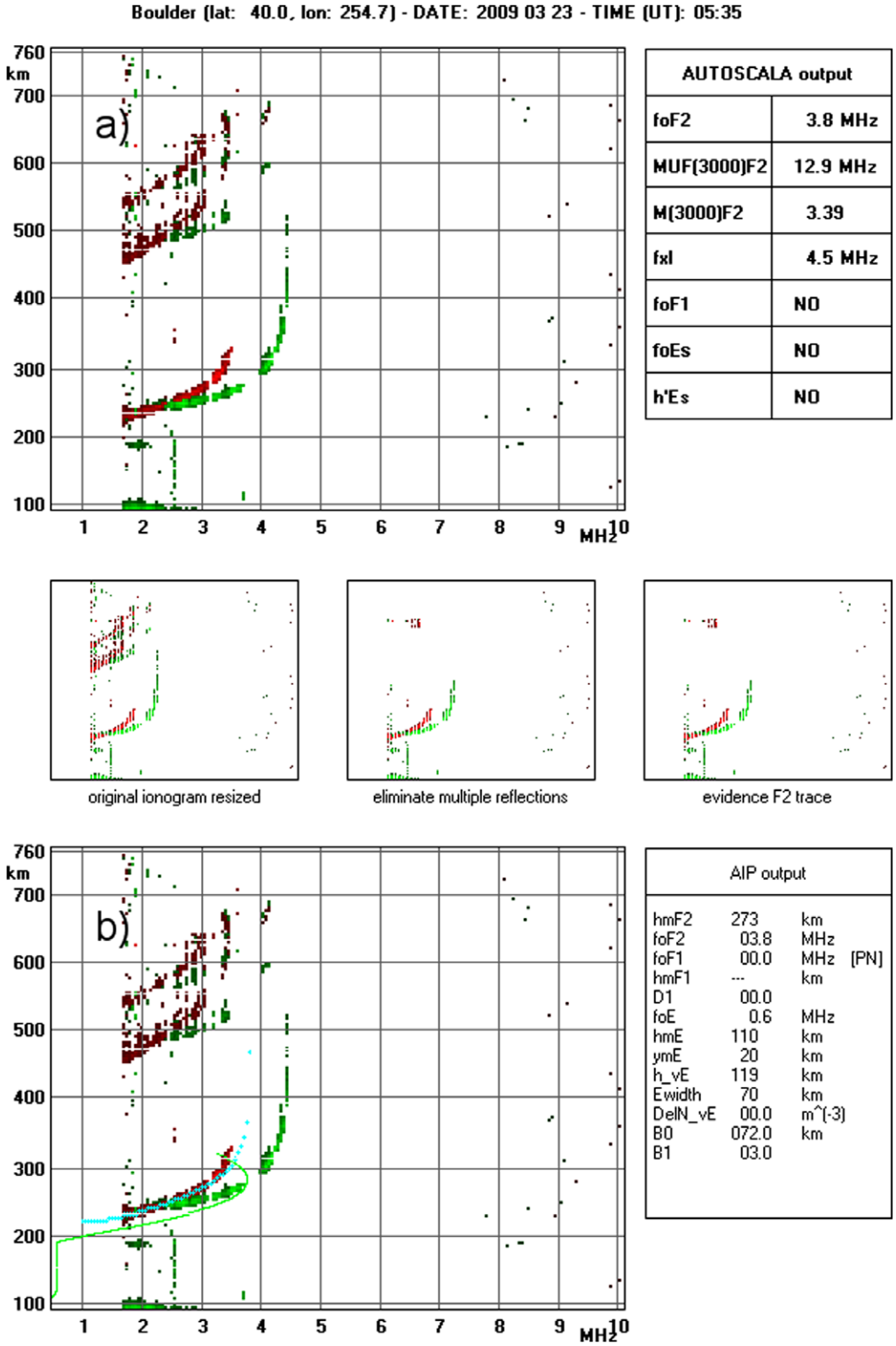

Fig. 1. (a) Ionogram recorded on 23 March 2009 at 5:35 UT by the VIPIR ionosonde installed at Boulder. The ordinary trace is obscured by interference, while the extraordinary component is clearly visible. The main ionospheric characteristics given as output by Autoscala are visible on the table "Autoscala output". (b) The same ionogram on which the reconstructed ordinary ray (light blue crosses) and the corresponding vertical electron density profile (in green) were drawn. In the table "AIP output" the parameters used by Autoscala to estimate the vertical electron density profile associated with the reconstructed ordinary trace. (For interpretation of the references to color in this figure legend, the reader is referred to the web version of this article.)

Once different parts of the ionogram trace have been automatically identified, in order to estimate the electron density profile, an iterative technique is used to best fit a 12 free parameter electron density profile model with the recorded ionogram (Scotto, 2009).

4. Analysis and results

The performances of Autoscala were tested on 8998 ionograms recorded by the VIPIR ionosonde at Boulder from 21 March to 9 April 2009, during quiet ionospheric condi-

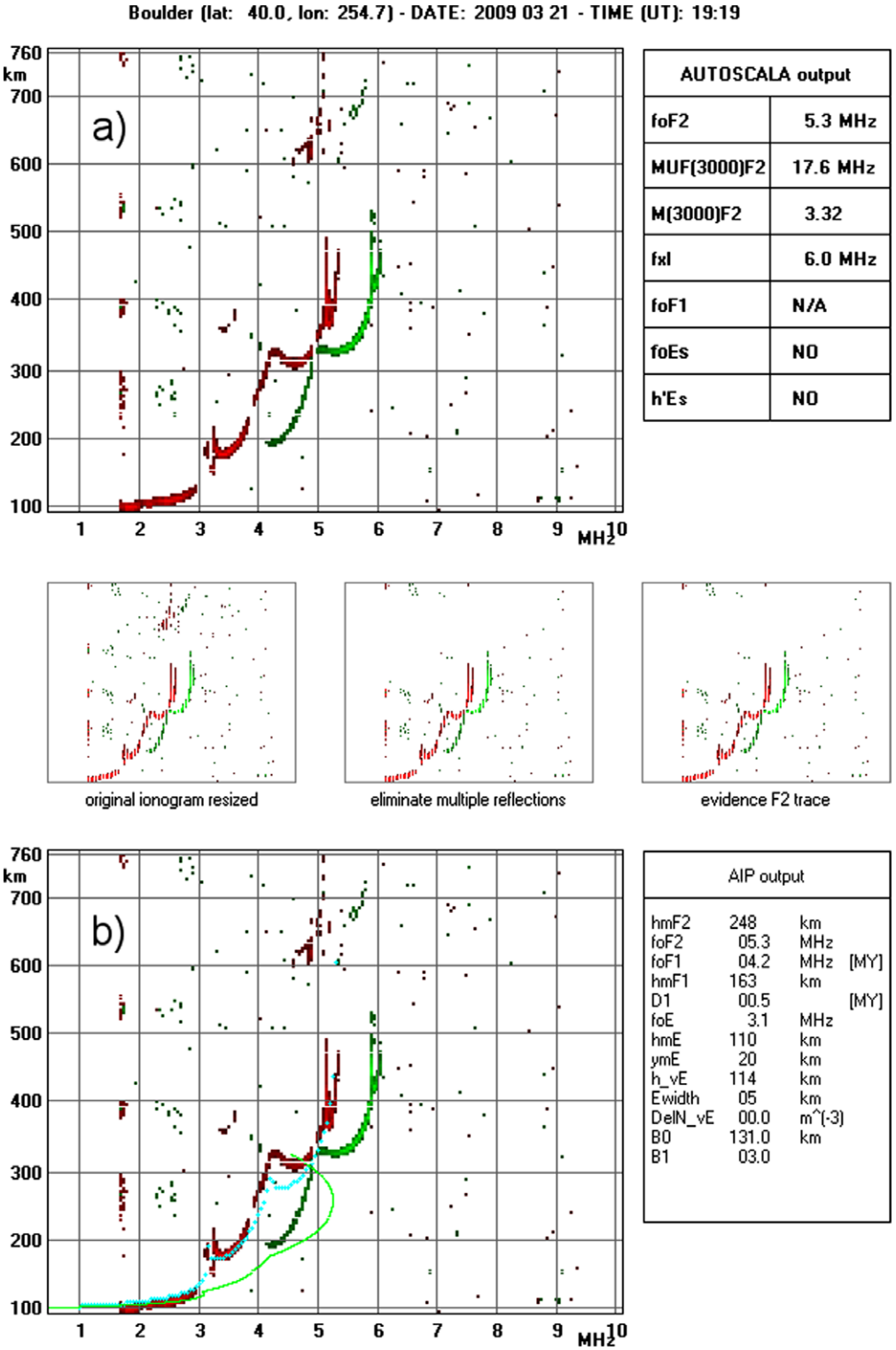

Fig. 2. (a) Ionogram recorded on 21 March 2009 at 19:19 UT by the VIPIR ionosonde installed at Boulder. The F trace consists of two pairs of the ordinary and extraordinary components. The main ionospheric characteristics given as output by Autoscala are visible on the table "Autoscala output". (b) The same as in Fig. 1.

tions, using as a reference the data obtained manually by a well experienced operator according to the International Union of Radio Science (URSI) standard.

The comparison was performed separately for the critical frequencies *fo*F2, *fo*F1, and *fo*Es, and for *MUF*(3000)F2 and *h*'Es.

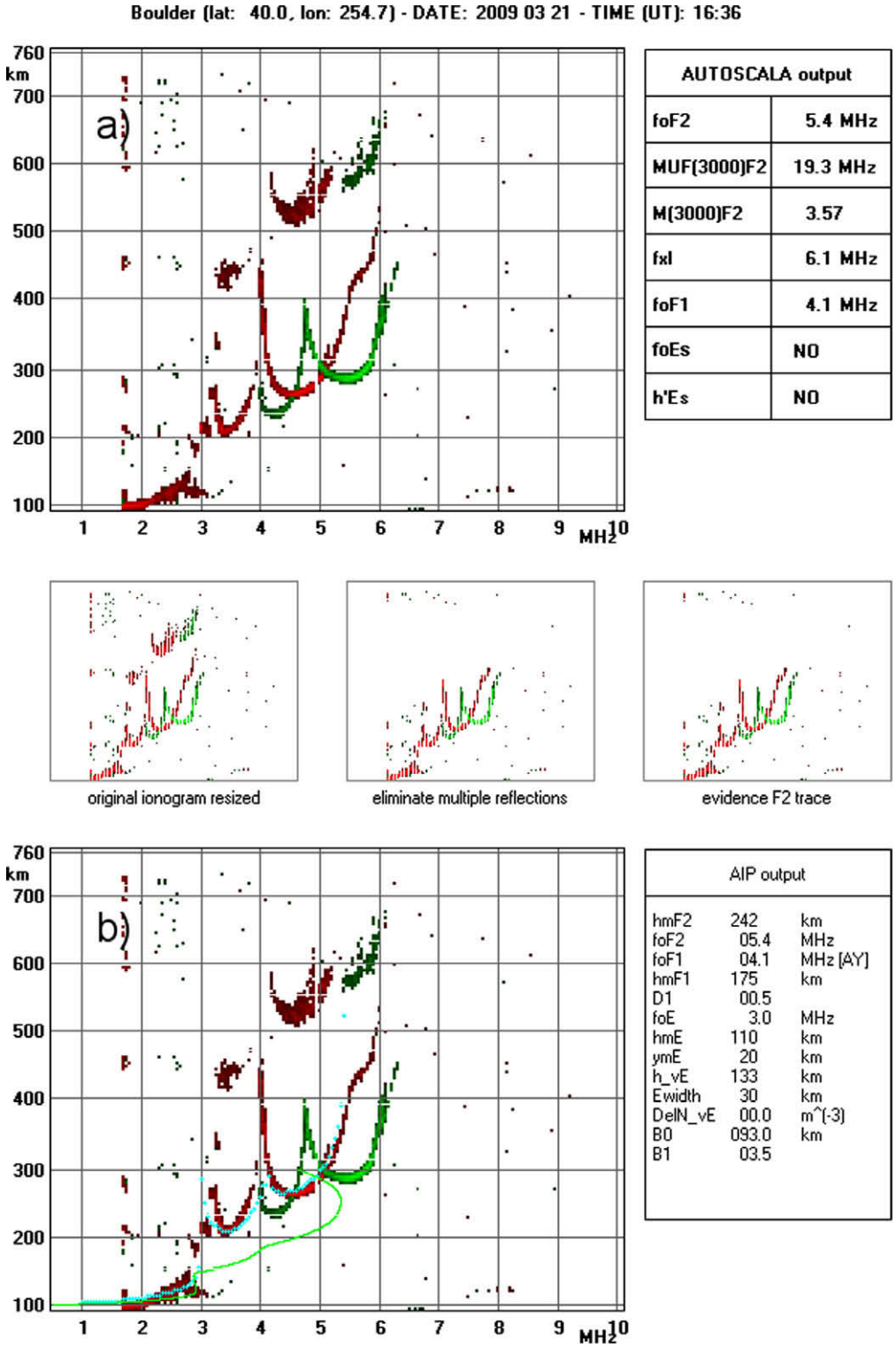

Fig. 3. (a) Ionogram recorded on 21 March 2009 at 16:36 UT by the VIPIR ionosonde installed at Boulder. An abnormal cusp is observed at the critical frequency of the F2 layer ordinary component. The main ionospheric characteristics given as output by Autoscala are visible on the table "Autoscala output". (b) The same as in Fig. 1.

4.1. Test for the foF2 characteristic

With reference to the processing dataset of 8998 ionograms, the following subsets were considered:

1. Subset *C* (definite values). Composed of ionograms for which the operator was able to scale *fo*F2 as a definite value, using neither descriptive nor qualifying letters.
2. Subset *D* (doubtful values). Composed of ionograms for which the operator scaled *fo*F2 as a doubtful value. This subset includes the following cases:
   a. the trace near the critical frequency is not clearly recorded owing to interference, or absorption;
   b. the ordinary trace is obscured by absorption, interference or blanketing while the extraordinary component is clearly visible (see Fig. 1); in these cases the URSI standard recommends deriving *fo*F2 of the ordinary trace from the extraordinary one.
3. Subset *F* (spread *F*). Composed of ionograms for which a spread F condition was observed.
4. Subset *V* (fork-shaped trace). Composed of ionograms for which the F trace consists of two pairs of the ordinary and extraordinary components (see Fig. 2); in these cases the URSI standard recommends deriving *fo*F2 from the higher frequency trace.
5. Subset *H* (stratification). Composed of ionograms for which an abnormal cusp (appearance of stratification) is observed at the critical frequency of the F2 layer ordinary component (see Fig. 3); usually the abnormal cusp is thinner than the main one and in these cases the URSI standard recommends deriving *fo*F2 from the main trace in lower frequencies rather than from the higher thin trace which might be a transient reflection.
6. Subset *U* (unscaleable). Composed of ionograms for which the operator was not able to observe the F2 trace for different reasons.

The results of the comparison are reported for each subset in Table 1. The very good O \ X separation performed by VIPIR allows Autoscala to reliably identify the trace, not only when it is very well defined, but also when F2 multiple reflections, Es multiple reflections, or spread F phenomena characterize the ionogram (see Figs. 4–7). On the contrary, an incorrect autoscaling behavior characterizes subset *U*, for which there are a large number of unacceptably scaled ionograms. This is due to the fact that in this first stage of testing, it was chosen to use an Autoscala version without including the routine for highlighting the F trace. As a consequence, Autoscala wrongly identifies a trace on ionograms characterized only by noise, as illustrated in Fig. 8. At this preliminary stage we chose not to apply such a filter because its application on very detailed ionograms, like the ones recorded by the VIPIR, results in a overall worsening of the available information with a

Table 1
The manually scaled *fo*F2 values are compared to the automatically scaled values obtained by Autoscala considering two different frequency intervals of accuracy, ±0.5 MHz and ±0.1 MHz. The comparison is performed separately for subsets *C*, *D*, *F*, *V*, *H*, and *U*. NS stands for not scaled ionograms, and S stands for scaled ionograms.

	Subset *C* (7467 ionograms)			Subset *D* (154 ionograms)			Subset *F* (18 ionograms)			Subset *V* (231 ionograms)			Subset *H* (12 ionograms)			Subset *U* (1116 ionograms)	
	⩽|0.5| MHz	>|0.5| MHz	NS	⩽|0.5| MHz	>|0.5| MHz	NS	⩽|0.5| MHz	>|0.5| MHz	NS	⩽|0.5| MHz	>|0.5| MHz	NS	⩽|0.5| MHz	>|0.5| MHz	NS	NS	S
Autoscala [%]	99.0	0.5	0.5	98.0	0	2.0	100.0	0	0	94.0	2.0	4.0	92.0	8.0	0	85.0	15.0
	⩽|0.1| MHz	>|0.1| MHz	NS	⩽|0.1| MHz	>|0.1| MHz	NS	⩽|0.1| MHz	>|0.1| MHz	NS	⩽|0.1| MHz	>|0.1| MHz	NS	⩽|0.1| MHz	>|0.1| MHz	NS	NS	S
Autoscala [%]	76.0	23.5	0.5	90.0	8.0	2.0	44.0	56.0	0	43.0	53.0	4.0	58.0	42.0	0	85.0	15.0

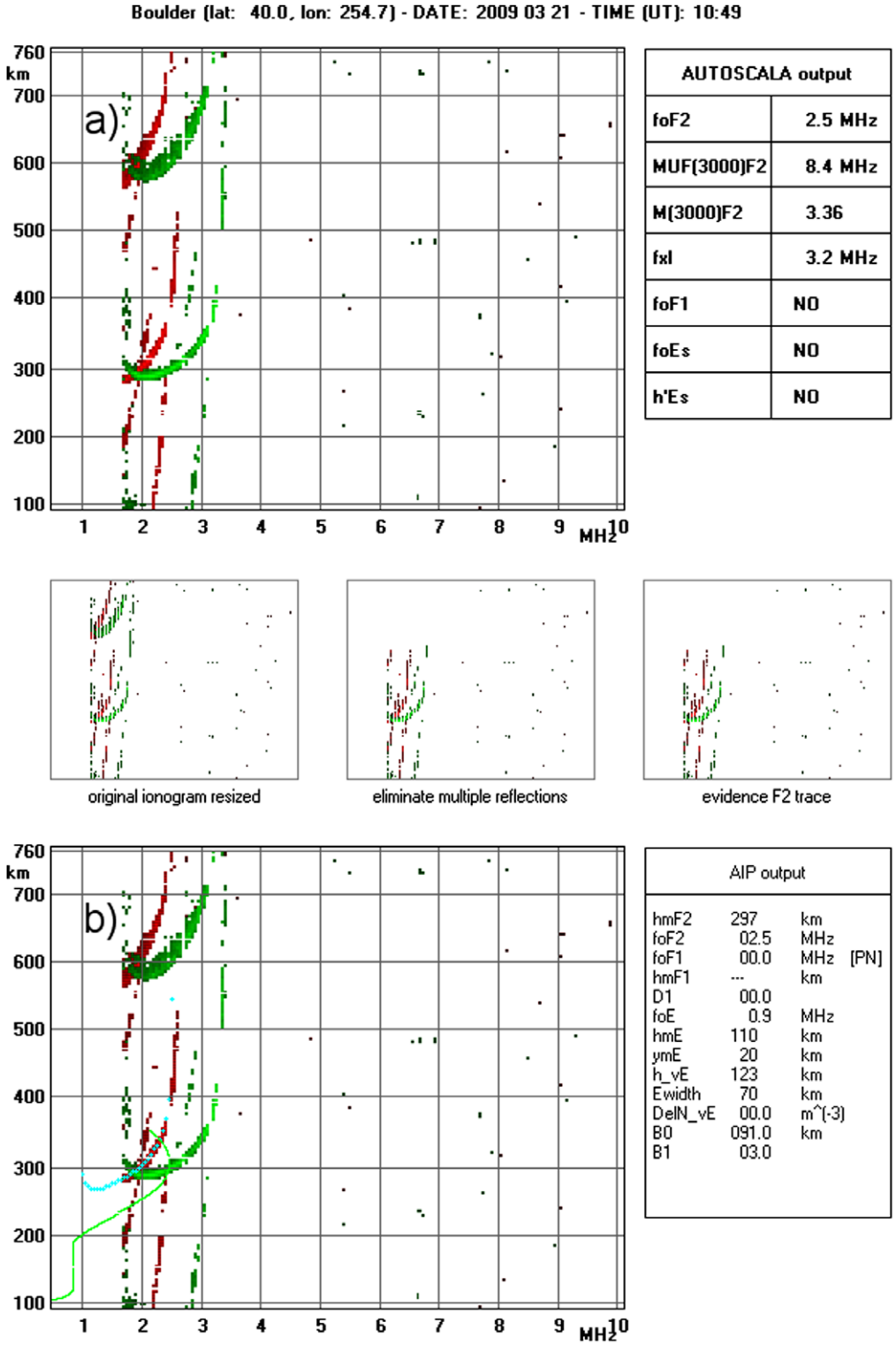

Fig. 4. (a) Ionogram recorded on 21 March 2009 at 10:49 UT by the VIPIR ionosonde installed at Boulder and characterized by F2 multiple reflections. The main ionospheric characteristics given as output by Autoscala are visible on the table "Autoscala output". (b) The same as in Fig. 1.

consequent decrease in the accuracy of the *fo*F2 value given as output (see Fig. 9). Hence, the application of this filter needs to be further investigated.

A summary of the *fo*F2 autoscaling accuracy compared to manual scaling is shown in form of histograms in Fig. 10.

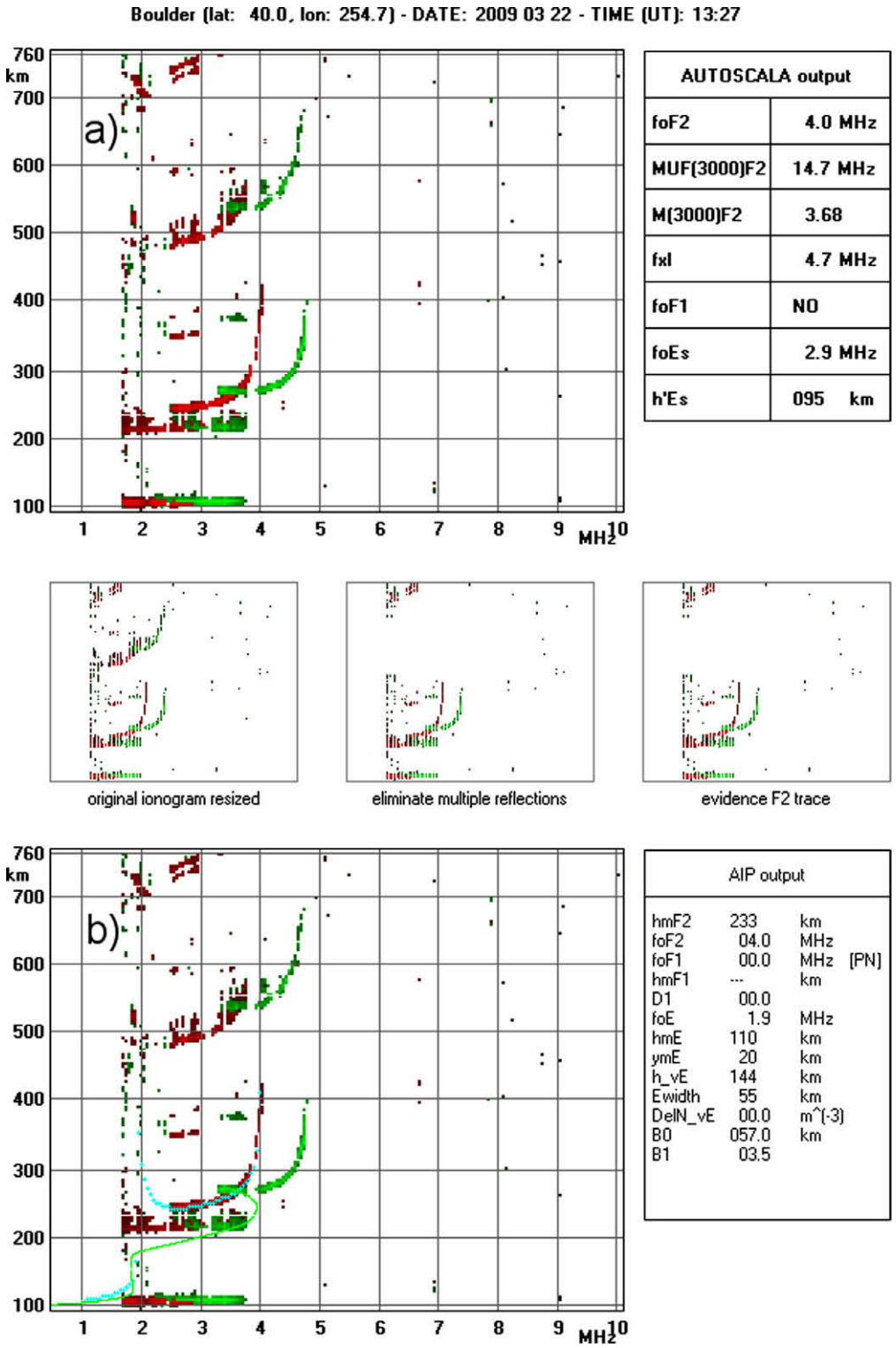

Fig. 5. (a) Ionogram recorded on 22 March 2009 at 13:27 UT by the VIPIR ionosonde installed at Boulder and characterized by Es multiple reflections. The main ionospheric characteristics given as output by Autoscala are visible on the table "Autoscala output". (b) The same as in Fig. 1.

4.2. Test for the MUF(3000)F2 characteristic

With reference to the processing data set of 8998 ionograms, the following three subsets were considered:

1. Subset *S*. Composed of ionograms belonging to subsets *C*, *D*, *V*, and *H* as defined in Section 4.1.
2. Subset *F* (spread *F*). Composed of ionograms for which a spread F condition was observed.

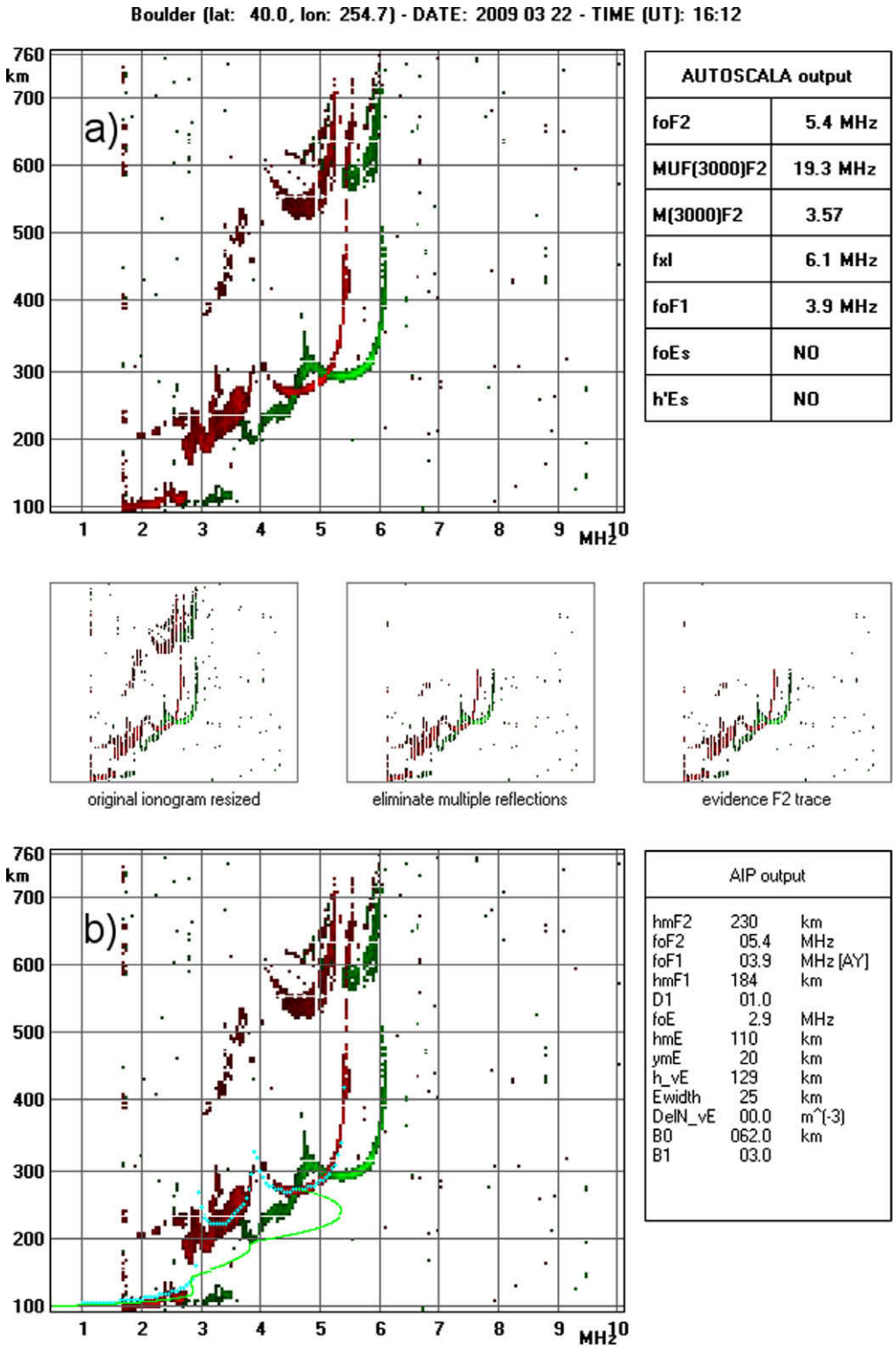

Fig. 6. (a) Ionogram recorded on 22 March 2009 at 16:12 UT by the VIPIR ionosonde installed at Boulder and characterized by a moderate spread of the F1 trace. The main ionospheric characteristics given as output by Autoscala are visible on the table "Autoscala output". (b) The same as in Fig. 1.

3. Subset *U* (unscaleable). Composed of ionograms for which the operator was not able to observe both the ordinary and the extraordinary trace for different reasons.

The results of the comparison are reported for each subset in Table 2.

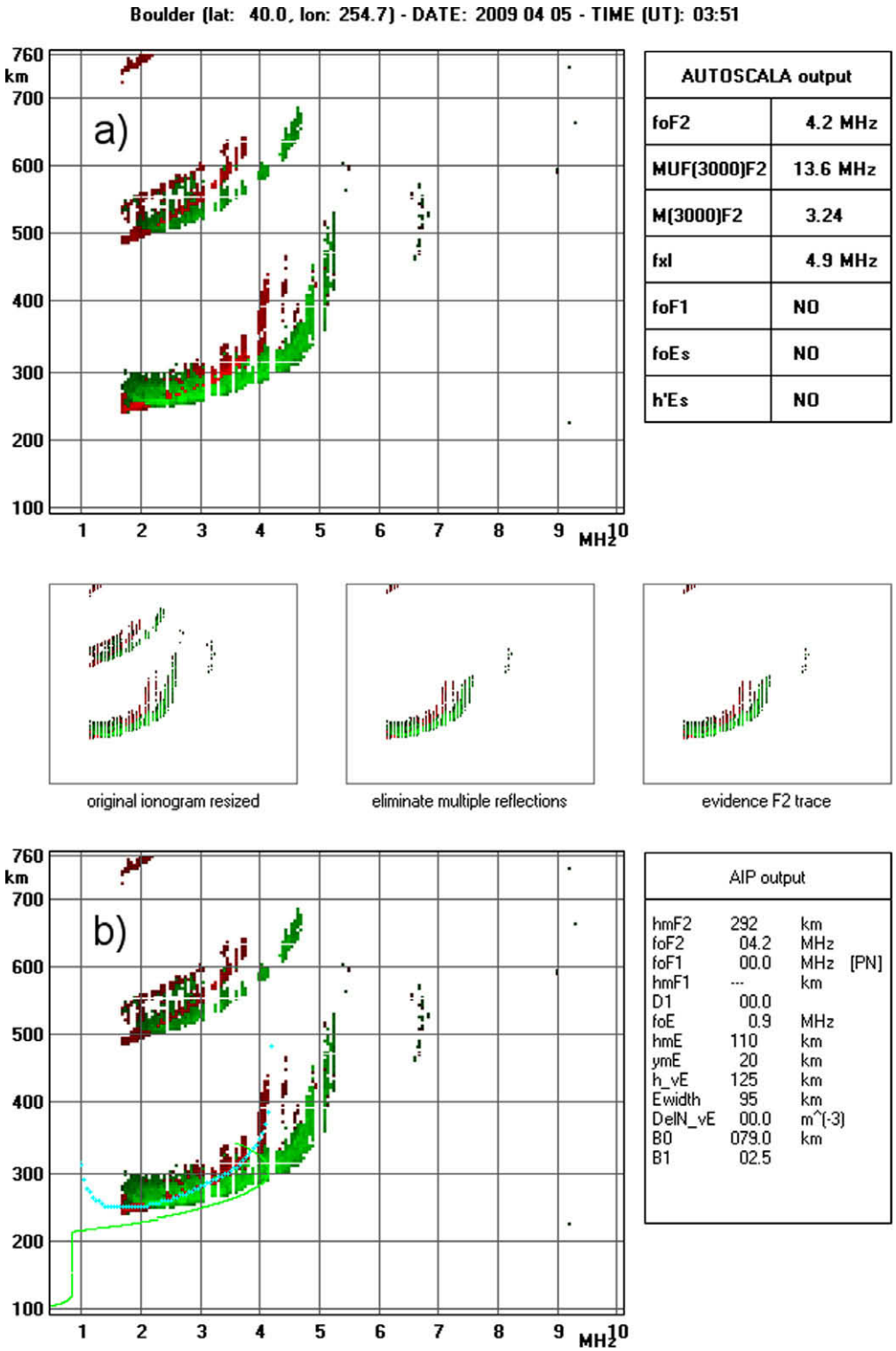

Fig. 7. (a) Ionogram recorded on 5 April 2009 at 03:51 UT by the VIPIR ionosonde installed at Boulder and characterized by spread F condition. The main ionospheric characteristics given as output by Autoscala are visible on the table "Autoscala output". (b) The same as in Fig. 1.

4.3. Test for the foF1 characteristic

With reference to the processing dataset of 8998 ionograms, the following subsets were considered:

1. Subset *C* (definite values). Composed of ionograms for which the F1 cusp is very clear and the operator was able to scale *fo*F1 as a definite value, using neither descriptive nor qualifying letters.

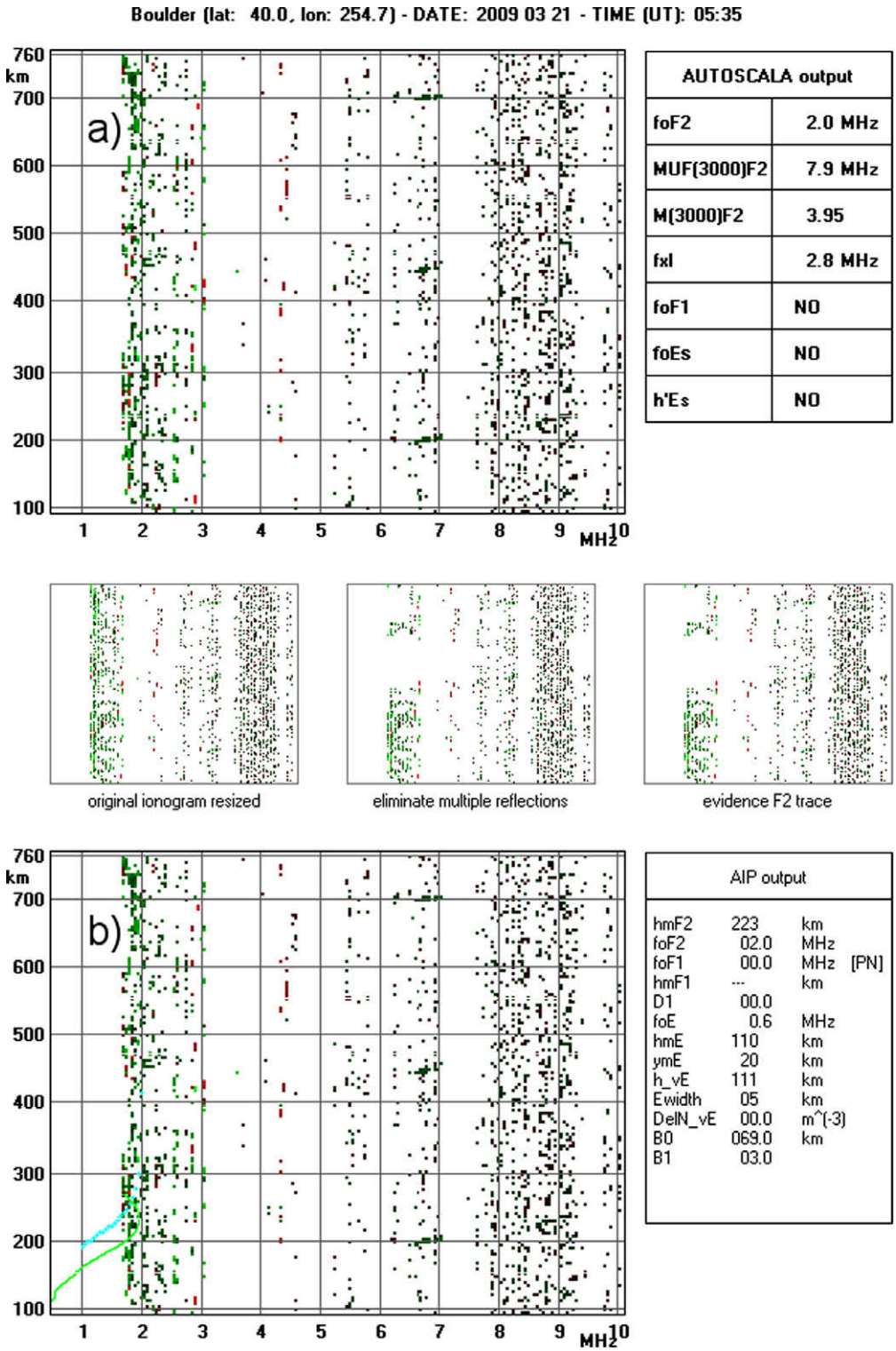

Fig. 8. (a) Ionogram recorded on 21 March 2009 at 05:35 UT by the VIPIR ionosonde installed at Boulder. The ionogram trace is completely absent due to interference. (b) The incorrect scaling performed by Autoscala that identified an F trace (light blue crosses) and estimated the corresponding vertical electron density profile (in green). (For interpretation of the references to color in this figure legend, the reader is referred to the web version of this article.)

2. Subset *UL* (doubtful values due to *L* condition). Composed of ionograms for which the F1 cusp is doubtful (see Fig. 11). For these cases the URSI standard suggests to express *fo*F1 as the transition frequency between the F1 and the F2 trace, followed by the descriptive letter *U* and the qualifying letter *L*.

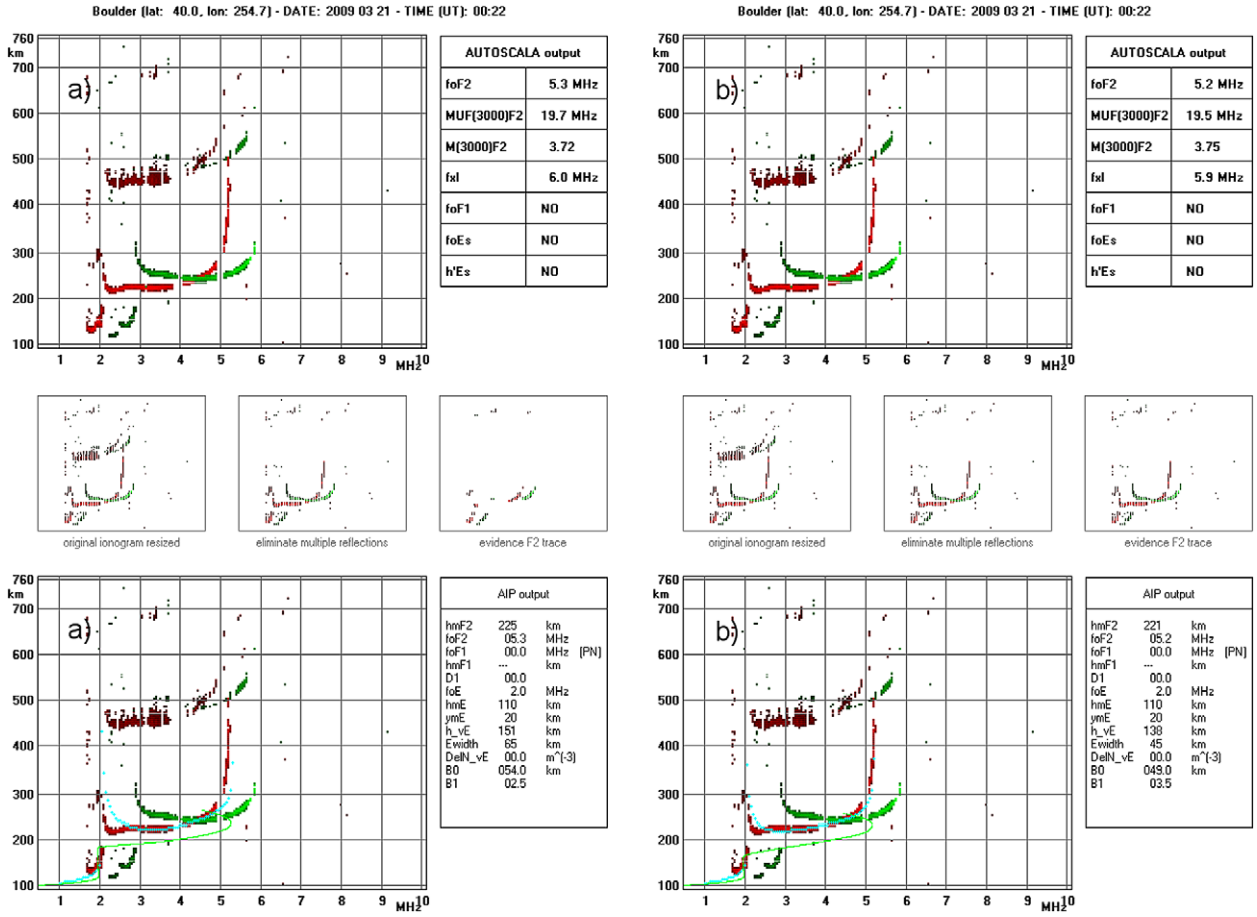

Fig. 9. Ionogram recorded on 21 March 2009 at 00:22 UT by the VIPIR ionosonde installed at Boulder and autoscaled by Autoscala (a) after applying the routine for highlighting the F trace and (b) without applying it.

3. Subset *L* (F1 layer not fully formed). Composed of ionograms for which the F1 layer is not fully formed and no clear cusp is observed between the F1 and F2 traces (see Fig. 12); for these ionograms the URSI standard suggests to express *fo*F1 only with the descriptive letter *L*.
4. Subset NP (F1 layer not present). Composed of ionograms for which the F1 trace is not present.

For each subset we considered:

a. The percentage of ionograms for which the software detected the F1 trace together with the percentages of acceptability of the corresponding *fo*F1 value;
b. The percentage of ionograms for which the software established that the ionogram information was sufficient to assume that the F1 trace was not present (the corresponding output is NO as in Fig. 11);
c. The percentage of ionograms for which the software considered the ionogram information insufficient to assess whether the F1 trace was present or not (the corresponding output is N/A as in Fig. 2).

The results of the comparison are reported for each subset in Table 3. It appears that the Autoscala performance is not so good as for *fo*F2, mostly for subset *C*. In order to improve the autoscaling of such ionograms the threshold characterizing the F1 routine (Pezzopane and Scotto, 2008) could be decreased but this issue needs to be further studied and carefully tested.

With regard to subset *UL*, Fig. 11 shows a case of an ionogram characterized by an L condition and belonging to subset *UL* for which Autoscala does not succeed in detecting the F1 layer giving NO as output for *fo*F1. As shown in Table 3, the F1 routine is fairly limited for this type of ionogram. This because at present the F1 routine tries to identify only the trace from the F1 cusp to the lowest virtual height of the F2 layer ordinary trace (Pezzopane and Scotto, 2008). The ionograms belonging to subset *UL* often present a practically flat shape of the trace on the high frequency side of the F1 ledge and this misleads the F1 routine of Autoscala. In order to avoid this kind of error, also the ionogram information coming from the trace on the low frequency side of the F1 cusp should be used, but this feature still needs to be developed.

A summary of the *fo*F1 autoscaling accuracy compared to manual scaling is shown in form of histograms in Fig. 13.

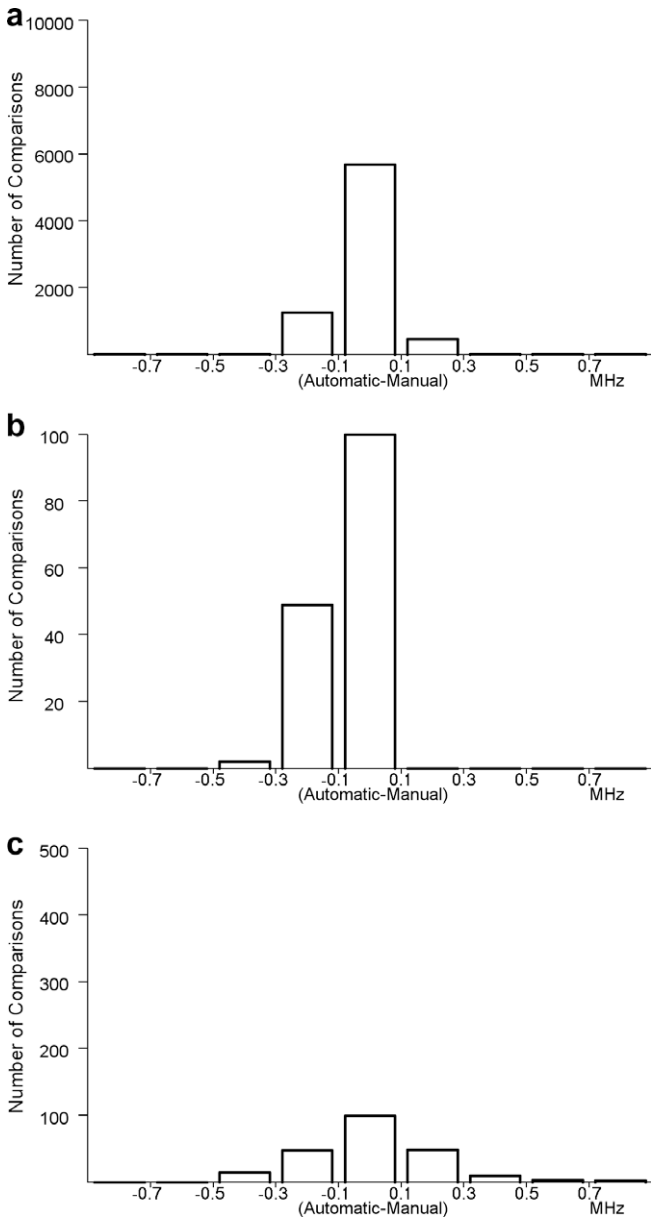

Fig. 10. Differences (Automatic-Manual) between the values of *fo*F2, for ionograms for which both Autoscala and the operator identified the F2 layer, for the different subsets (a) definite values [C] , (b) doubtful values [D], and (c) forked traces [V].

4.4. Test for the foEs and h'Es characteristics

With reference to the processing dataset of 8998 ionograms, the following subsets were considered:

1. Subset *C* (definite values). Composed of ionograms for which the operator observed an Es layer and gave as output a value for *fo*Es and for *h*'Es.
2. Subset *NP* (Es layer not present). Composed of ionograms for which the operator did not observe an Es layer.

The results of the comparison are reported for *fo*Es and for *h*'Es in Tables 4 and 5 respectively. These tables show that for the cases in which Autoscala detected the Es layer both *fo*Es and *h*'Es are reliably estimated. On the other hand we have to notice that a high percentage of ionograms having Es features have escaped detection by Autoscala. This suggests that further work is necessary to improve the performance of Es automatic scaling routine. It is worthwhile to note that the routine performs better when *fo*Es is high, while this is verified for a few cases in the database (only 25 out of 8998 have *fo*Es >4.0 MHz).

5. Discussion

Ionograms recorded by VIPIR ionosonde are definitely well defined and accurate. This high definition introduces a variety of traces not so easily recordable with other ionosondes, like for instance the "fork" ionogram shown in Fig. 2, and facilitates autoscaling system. In fact this strong point of VIPIR made it possible to lower the thresholds characterizing the Autoscala algorithm (Pezzopane and Scotto, 2007), with a consequent improvement of the accuracy percentages of autoscaled output.

Comparing the results shown in the previous paragraphs with those obtained by applying Autoscala to other ionosondes the following considerations can be done:

(a) In comparison to the results obtained by applying Autoscala to the AIS-INGV ionosonde installed at Gibilmanna, Italy, (Pezzopane and Scotto, 2004) and the AIS Parus ionosonde installed at Moscow, Russia (Krasheninnikov et al., in press), which are both not able to tag differently the ordinary and the extraordinary rays, the results shown in this paper appear more reliable and accurate.
(b) In comparison to the results obtained by applying Autoscala to the VISRC2 ionosonde installed at Warsaw, Poland (Pezzopane et al., 2008), which is instead able to tag differently the ordinary and the extraordinary rays, the results shown in this paper

Table 2
The manually scaled *MUF*(3000)F2 values are compared to the automatically scaled values obtained by Autoscala considering two different frequency intervals of accuracy, ±2.5 MHz and ±0.5 MHz. The comparison is performed separately for subsets *S*, *F*, and *U*. NS stands for Not Scaled ionograms, and S stands for Scaled ionograms.

	Subset *S* (7864 ionograms)			Subset *F* (18 ionograms)			Subset *U* (1116 ionograms)	
	⩽|2.5| MHz	>|2.5| MHz	NS	⩽|2.5| MHz	>|2.5| MHz	NS	NS	S
Autoscala [%]	99.1	0.4	0.5	100.0	0	0	85.0	15.0
	⩽|0.5| MHz	>|0.5| MHz	NS	⩽|0.5| MHz	>|0.5| MHz	NS	NS	S
Autoscala [%]	75.6	23.9	0.5	61.0	39.0	0	85.0	15.0

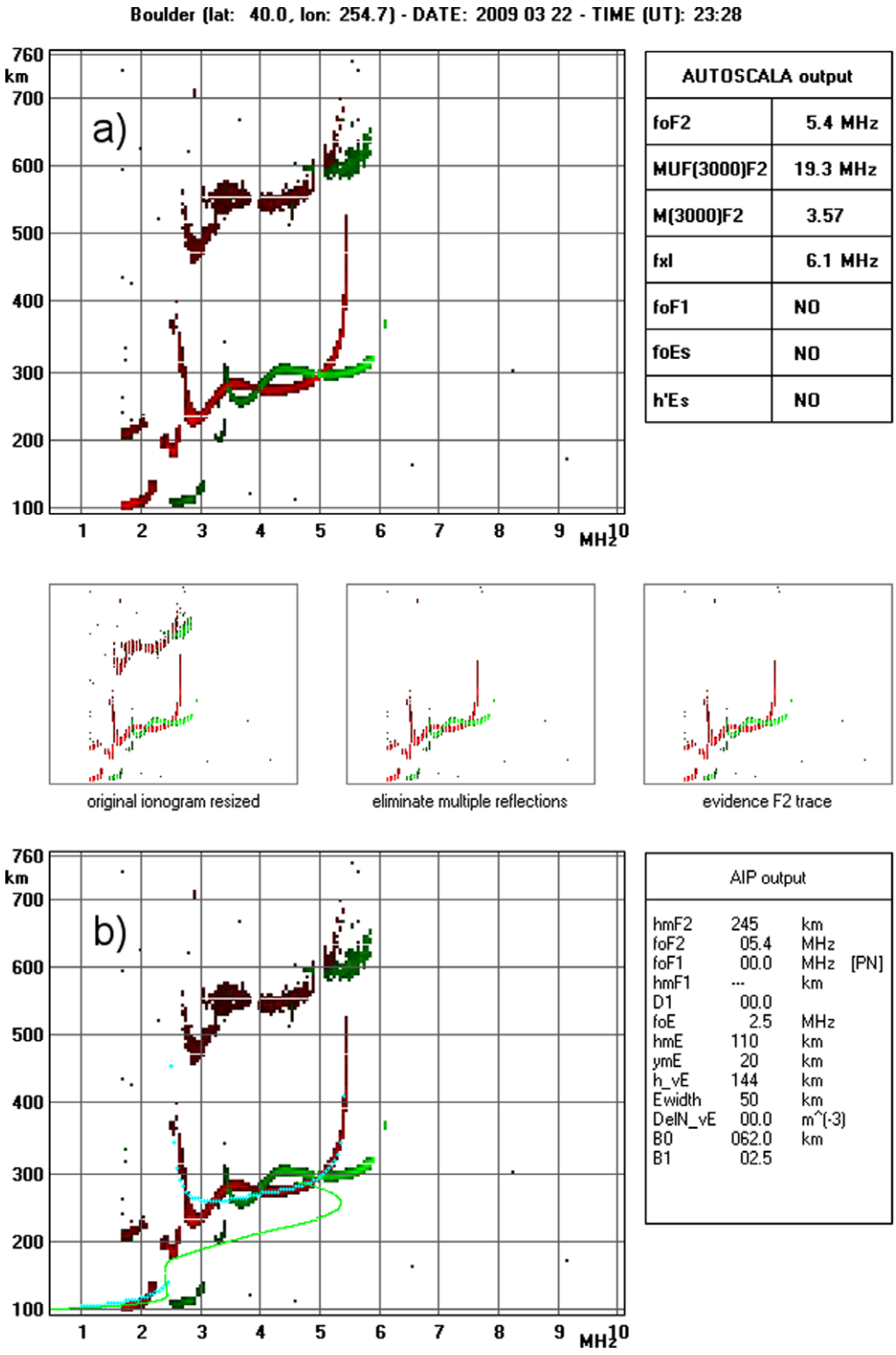

Fig. 11. (a) Ionogram recorded on 22 March 2009 at 23:28 UT by the VIPIR ionosonde installed at Boulder. The F1 cusp is neither typical nor clear. The main ionospheric characteristics given as output by Autoscala are visible on the table "Autoscala output". (b) The same as Fig. 1.

still appear more reliable and accurate, as confirmation of a good O/X mode separation made by the VIPIR ionosonde.

(c) The histograms shown in Figs, 10 and 13, as already observed in the analyses carried out on ionograms recorded by other equipments (Krashenninikov et al., in press; Pezzopane et al., 2008; Pezzopane and Scotto, 2004), discloses an asymmetrical distribution of errors. This feature, characterizing mostly ionograms belonging to subset *D*, is strictly related to the extrapolation process performed by Autoscala when the asymptotical vertical

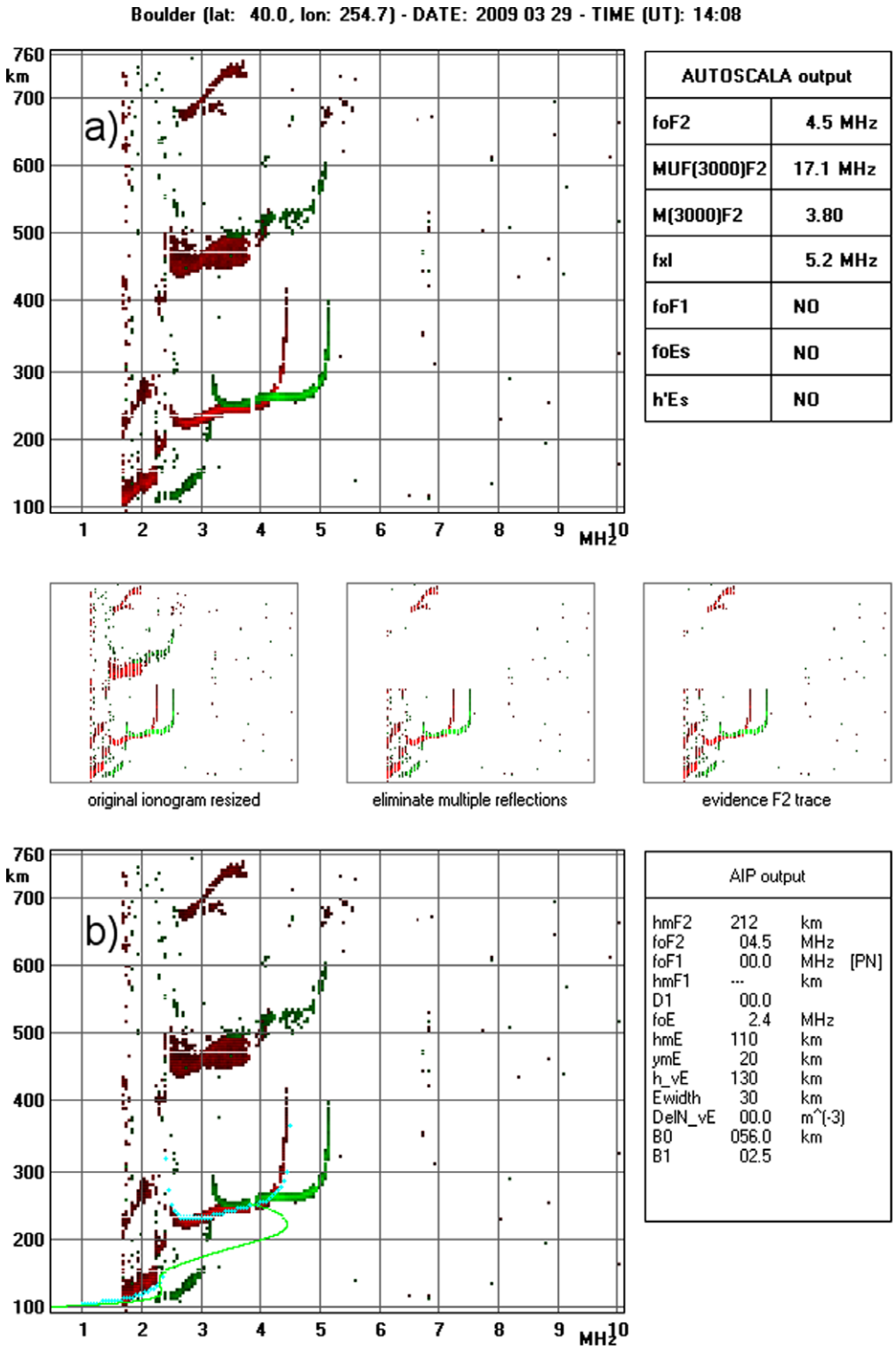

Fig. 12. (a) Ionogram recorded on 29 March 2009 at 14:08 UT by the VIPIR ionosonde installed at Boulder. The F1 layer is not fully formed and no clear cusp is observed between the F1 and F2 traces. The main ionospheric characteristics given as output by Autoscala are visible on the table "Autoscala output". (b) The same as Fig. 1.

part (referring to F1 and F2 layers) or the final part (referring to the Es layer) of the trace are not well defined. In fact this procedure in these cases may introduce a small underestimation of the automatically obtained critical frequency compared to the one manually scaled.

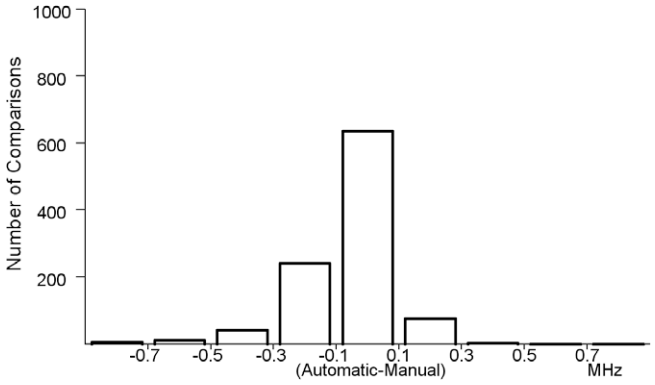

Fig. 13. Differences (Automatic-Manual) between the values of *fo*F1, for ionograms for which both Autoscala and the operator identified the F1 layer, for definite manually scaled values (subset *C*).

(d) The median errors reported in Table 6 spotlight the same asymmetrical distribution of errors as they have been illustrated at the above point.

6. Conclusions

A new research ionosonde is operating at Boulder, CO, USA and is producing a very large number of high quality ionograms which need to be reduced to standard URSI characteristics. The new ionosonde data often reveal ionogram features that are difficult to place within standard URSI categories. The ionogram analysis software Autoscala has been applied to these data. Minor adaptations of the ionogram data format were needed to interface the instrument to the analysis software. The ability and accuracy of Autoscala to extract standard ionogram characteristics of *fo*F2, *MUF*(3000)F2, *fo*F1, *foEs* and *h*'Es were carefully compared to manually determined values.

Although Autoscala accuracy is good compared to other analyses performed on ionograms recorded by other equipments, improvements mostly concerning sporadic-E and F1 layer detection are desirable. Automatic ionogram interpretation remains a scientific challenge.

Table 4
The manually scaled *fo*Es values are compared to the automatically scaled values obtained by Autoscala considering two different frequency intervals of accuracy, ±0.5 MHz and ±0.1 MHz. The comparison is performed separately for subsets *C*, and *NP*.

	Autoscala		
	Subset *C* (119 ionograms)		Subset *NP* (8879 ionograms)
Es layer detected [%]	⩽|0.5| MHz 80.2 ⩽|0.1| MHz 27.7	>|0.5| MHz 19.8 >|0.1| MHz 72.3	4.9
Es layer not detected [%]	10.9		95.1

Table 5
The manually scaled *h*'Es values are compared to the automatically scaled values obtained by Autoscala considering two different height intervals of accuracy, ±9 km and ±3 km. The comparison is performed separately for subsets *C*, and *NP*.

	Autoscala		
	Subset *C* (119 ionograms)		Subset *NP* (8879 ionograms)
Es layer detected [%]	⩽|9| km 98.3 ⩽|3| km 88.2	>|9| km 1.7 >|3| km 11.8	4.9
Es layer not detected [%]	10.9		95.1

Table 6
Median errors of critical frequencies *fo*F2, *fo*F1, and *fo*Es automatically scaled values compared to the manually ones.

	*fo*Es	*fo*F1	*fo*F2				
			Subset *C*	Subset *D*	Subset *F*	Subset *V*	Subset *H*
Median error [MHz]	0.2	−0.03	0	−0.1	0.1	0	0

Table 3
The manually scaled *fo*F1 values are compared to the automatically scaled values obtained by Autoscala considering two different frequency intervals of accuracy, ±0.5 MHz and ±0.1 MHz. The comparison is performed separately for subsets *C*, *UL*, *L*, and *NP*.

	Autoscala					
	Subset *C* (2939 ionograms)		Subset *UL* (75 ionograms)		Subset *L* (846 ionograms)	Subset *NP* (5138 ionograms)
F1 layer detected [%]	⩽|0.5| MHz 98.3 ⩽|0.1| MHz 65.1	>|0.5| MHz 1.7 >|0.1| MHz 34.1	⩽|0.5| MHz 0 ⩽|0.1| MHz 0	>|0.5| MHz 0 >|0.1| MHz 0	0	0
Sufficient information to state that the F1 layer is not present [%]	14.3		62.7		81.9	91.2
Insufficient information to state whether the F1 layer is present or not [%]	51.2		37.3		18.1	8.8

References

Grubb, R.N. The NOAA SEL HF Radar System (Ionospheric Sounder). NOAA Technical Memorandum ERL SEL-55, October 1979.

Grubb, R.N., Livingston, R., Bullett, T.W. A new general purpose high performance HF Radar. XXIX URSI General Assembly, Chicago, IL, USA, 2008.

Krasheninnikov, I., Pezzopane, M., Scotto, C. Application of Autoscala to ionograms recorded by the AIS-Parus ionosonde. Comp. Geosc. 30, in press.

Pezzopane, M. Interpre: a Windows software for semiautomatic scaling of ionospheric parameters from ionograms. Comp. Geosc. 30, 125–130, 2004.

Pezzopane, M., Scotto, C. Software for the automatic scaling of critical frequency foF2 and MUF(3000)F2 from ionograms applied at the Ionospheric Observatory of Gibilmanna, Ann. Geophys. Italy, 47(6), 1783–1790, 2004.

Pezzopane, M., Scotto, C. The INGV software for the automatic scaling of foF2 and MUF(3000)F2 from ionograms: a performance comparison with ARTIST 4.01 from Rome data.. J. Atmos. Solar-Terr. Phys. 67, 1063–1073, 2005.

Pezzopane, M., Scotto, C. The Automatic Scaling of Critical Frequency foF2 and MUF(3000)F2: a comparison between Autoscala and ARTIST 4.5 on Rome data.. Radio Sci. 42, RS4003, doi:10.1029/2006RS003581, 2007.

Pezzopane, M., Scotto, C. A method for automatic scaling of F1 critical frequency from ionograms. Radio Sci. 43, RS2S91, doi:10.1029/2007RS003723, 2008.

Pezzopane, M., Scotto, C., Stanislawska, I., Juchnikowski, G., 2008, Autoscala applied at the Ionospheric Station of Warsaw, INAG (Ionosonde Network Advisory Group) Bulletin 69, Available from <http://www.ips.gov.au/IPSHosted/INAG/web-69/index.html>.

Piggott, W.R, Rawer, K. URSI Handbook of Ionogram Interpretation and Reduction. Rept. UAG-23a, WDC-A for STP, Boulder, CO, USA, 1972.

Scotto, C., Pezzopane, M. A software for automatic scaling of foF2 and MUF(3000)F2 from ionograms. In: Proceedings of URSI 2002, Maastricht, 17–24 August, 2002 (on CD).

Scotto, C., Pezzopane, M. A method for automatic scaling of sporadic E layers from ionograms. Radio Sci. 42, RS2012, doi:10.1029/2006RS003461, 2007.

Scotto, C., Pezzopane, M. Removing multiple reflections from the F2 layer to improve Autoscala performance. J. Atmos. Solar-Terr. Phys. 70, 1929–1934, doi:10.1016/j.jastp.2008.05.012, 2008.

Scotto, C. Electron density profile calculation technique for Autoscala ionogram analysis. Adv. Space Res. 44 (6), doi:10.1016/j.asr.2009.04.037, 2009.

Wright, J.W., Pitteway, M.L.V. Real-time data acquisition and interpretation capabilities of the Dynasonde 1. Data acquisition and real-time display. Radio Sci. 14, 815–825, 1979a.

Wright, J.W., Pitteway, M.L.V. Real-time data acquisition and interpretation capabilities of the Dynasonde 2. Determination of magnetoionic mode and echolocation using a small spaced receiving array. Radio Sci. 14, 827–835, 1979b.

Wright, J.W., Bullett, T.W. The applicability of advanced ionosondes to the IRI. Adv. Space Res., V31, 775-780, ISSN 0273-1177, doi: 10.1016/S0273-1177(03)00052-8, 2003.